frontiers | Frontiers in Physiology

ORIGINAL RESEARCH
published: 05 July 2022
doi: 10.3389/fphys.2022.904664

Effects of Mexiletine on a Race-specific Mutation in $Na_v1.5$ Associated With Long QT Syndrome

Xin Wu[1], *Yawei Li*[2] *and Liang Hong*[1]*

[1]Department of Medicine, University of Illinois at Chicago, Chicago, IL, United States, [2]Department of Preventive Medicine, Northwestern University, Chicago, IL, United States

The voltage-gated sodium channel $Na_v1.5$ plays an essential role in the generation and propagation of action potential in cardiomyocytes. Mutations in $Na_v1.5$ have been associated with LQT syndrome, Brugada syndrome, and sudden arrhythmia death syndrome. Genetic studies showed that $Na_v1.5$ mutations vary across race-ethnic groups. Here we investigated an Asian-specific mutation $Na_v1.5$-P1090L associated with LQT syndrome. We found that $Na_v1.5$-P1090L mutation perturbed the sodium channel function. It altered the gating process of the channel and exhibited an enhanced window current. Treatment with mexiletine reversed the depolarization shift of the steady-state inactivation produced by P1090L. Mexiletine also modified the recovery from steady-state inactivation and the development of inactivation of P1090L. It rescued the dysfunctional inactivation of P1090L and reduced the P1090L channel's availability.

Keywords: voltage-gated sodium channel, Nav1.5, LQT syndrome, electrophysiology, patch clamp

OPEN ACCESS

Edited by:
Yanmin Zhang,
Xi'an Jiaotong University, China

Reviewed by:
Kamalan Jeevaratnam,
University of Surrey, United Kingdom
Anamika Bhargava,
Indian Institute of Technology Hyderabad, India
Yang Yan,
The First Affiliated Hospital of Xi'an Jiaotong University, China

***Correspondence:**
Liang Hong
hong2004@uic.edu

Specialty section:
This article was submitted to Cardiac Electrophysiology, a section of the journal Frontiers in Physiology

Received: *25 March 2022*
Accepted: *14 June 2022*
Published: *05 July 2022*

Citation:
Wu X, Li Y and Hong L (2022) Effects of Mexiletine on a Race-specific Mutation in $Na_v1.5$ Associated With Long QT Syndrome. Front. Physiol. 13:904664. doi: 10.3389/fphys.2022.904664

INTRODUCTION

Long QT syndrome (LQTS) is a heart rhythm disorder and increases risk for life-threatening sudden cardiac arrest (Napolitano et al., 2005; Ware et al., 2012). It is an inherited arrhythmia associated with ion channel mutations (Grant et al., 2002; Kapa et al., 2009; Chiu et al., 2012; Wilde and Amin, 2018).

The voltage-gated sodium channel $Na_v1.5$, encoded by SCN5A, plays a critical role in the fast depolarization of the cardiac action potential duration (APD) (Dong et al., 2020; Wu and Hong, 2021). Genetic mutations in $Na_v1.5$ linked with long QT syndrome type 3 (LQTS3) affected channel's function and remodeled ventricular APD (Bankston et al., 2007; Wilde and Amin, 2018). Some $Na_v1.5$ mutations have been shown to be race-specific. It was reported that $Na_v1.5$ mutations R34C and S1103Y were common variants in black cohort; and R1193Q and P1090L were observed predominantly among Asian patients (Ackerman et al., 2004). Although epidemiological research provided important insights into $Na_v1.5$ mutations, the role of some race-specific mutations in LQTS remained unclear.

Here we investigated an Asian-specific mutation $Na_v1.5$-P1090L associated with LQTS. The $Na_v1.5$ mutation P1090L was first reported to be linked with familial long QT syndrome in Japanese population (Iwasa et al., 2000). It was identified as an ethnic-specific variant in Asians (Ackerman et al., 2004). The $Na_v1.5$-P1090L has also been associated with Brugada syndrome, sudden infant death syndrome, sick sinus syndrome, and other severe arrhythmia (Ackerman et al., 2004; Lai et al., 2005; Tan et al., 2005; Shan et al., 2008; Zhang et al., 2008; Nakajima et al., 2011; Chiu et al., 2012) (**Table 1**). To explore the role of the P1090L in the LQTS, we characterized effects of the mutation on the channel function. We showed that P1090L perturbed the gating process of the sodium channel. It generated a larger window current associated with a gain-of-function mechanism underlying LQTS. We then studied effects of a targeted drug on the $Na_v1.5$-P1090L mutation.

TABLE 1 | Summary of citations for the $Na_v1.5$ mutation P1090L associated with cardiac arrhythmias.

Nav1.5 Variant	Change in Nucleotide	Phenotype	References
P1090L	c. 3269C > T	Long QT syndrome	Iwasa et al. (2000)
		Brugada/Long QT syndrome	Ackerman et al. (2004)
		Arrhythmia	Tan et al. (2005)
		Long QT syndrome	Lai et al. (2005)
		Premature ventricular contraction/Sick sinus syndrome	Shan et al. (2008)
		Arrhythmia	Zhang et al. (2008)
		Brugada syndrome	Nakajima et al. (2011)
		Long QT syndrome	Chiu et al. (2012)

MATERIALS AND METHODS

Cell Culture and $Na_v1.5$ Transfection

HEK-293T cell lines (Sigma-Aldrich, St. Louis, United States) were used to express human $Na_v1.5$ wild-type (WT) and mutation P1090L. The cells were reseeded on coverslips in 6-well plates containing Dulbecco modified Eagle's medium (DMEM, Invitrogen) supplemented with 10% fetal bovine serum (Invitrogen), 100 U/mL penicillin, and 100 μg/ml streptomycin at 37°C under 5% CO_2. After growth to ~80% confluence, cells were transiently transfected with $Na_v1.5$ cDNA plasmids. The pRc/CMV plasmid containing the sequence of the human $Na_v1.5$ channel was kindly provided by Dr Alfred L. George Jr (Northwestern University, Chicago, IL, United States). Single-point mutation of P1090L in pRc/CMV-h$Na_v1.5$ was introduced with standard PCR techniques. The mutation was introduced to the template plasmid using primers in a PCR protocol. The PCR cycles were initiated at 98°C for 1.5 min, followed by 25 amplification cycles. Each amplification cycle consisted of 98°C (20 s), 60°C (30 s), and 72°C (5 min). The cycles were finished with an extension step at 72°C for 15 min, followed by 4°C for 30 min. The template plasmid was removed using DpnI (NEB, R0176S), and Stbl2 competent cells (Invitrogen, 10268019) were transformed with the PCR product. Plasmids were isolated from Stbl2 cells with resulting colonies using QIAprep Spin Miniprep Kit (Qiagen, 27106). The mutation confirmed by the DNA sequencing was used for subsequent transfection.

The HEK-293T cells were transiently transfected with 2 μg of the cDNA encoding $Na_v1.5$ WT or P1090L mutation and 0.25 μg of a plasmid encoding enhanced green fluorescent protein (GFP) using Lipofectamine 3000 reagent (Invitrogen; Thermo Fisher Scientific, Inc., United States) according to the manufacturer's protocol. The mixture was then added to the culture dish and the cells were incubated at 37°C for 24 h before the electrophysiology studies were conducted. A coverslip with HEK-293T cells was placed in a recording chamber containing bath solution on the stage of a fluorescence microscope (Olympus, Japan), and the transfected cells identified by the fluorescent signal emitted from GFP were used for electrophysiological measurements. Patch clamp experiments were conducted 24–48 h after transfection.

Electrophysiological Measurements and Analysis

Patch clamp measurements were performed in whole-cell configuration using an Axopatch 200B amplifier controlled by pClamp11 software through an Axon Digidata 1550B system (Molecular Devices, United States). The extracellular solution contained 130 mM NaCl, 5 mM KCl, 1 mM $MgCl_2$, 2 mM $CaCl_2$, 10 mM HEPES, adjusted to pH 7.4 with NaOH. The intracellular solution contained 120 mM CsF, 15 mM CsCl, 20 mM NaCl, 2 mM EGTA and 5 mM HEPES, adjusted to pH 7.3 with CsOH. All measurements were performed at 22 ± 3°C. Pipettes had 2–4 MΩ access resistance.

The activation G-V curves were fitted by the Boltzmann equation, as previously explained (Kim et al., 2014; Hong et al., 2020): $G/G_{max} = 1/(1 + \exp(V\text{-}V_{1/2})/k)$, where G/G_{max} is the relative conductance normalized by the maximal conductance, $V_{1/2}$ is the potential of half activation, V is test pulse, and k is the Boltzmann coefficient. Steady-state inactivation curves were fitted by the Boltzmann equation: $I/I_{max} = 1/(1 + \exp(V\text{-}V_{1/2})/k)$, where I/I_{max} is the relative conductance normalized by the maximal conductance, $V_{1/2}$ is half-maximal inactivation, V is test pulse, and k is the Boltzmann coefficient.

Exponential functions of the form $y = y0+A(1\text{-}\exp[-t/\tau])$ were fitted to development curves to determine time constant (τ_{dev}), where y0 is the offset and A is amplitude. The double exponential functions of the form $y = A1(1\text{-}\exp[-t/\tau1])+A2(1\text{-}\exp[-t/\tau2])$ were fitted to recovery curves to determine time constants ($\tau_{rec,f}$ and $\tau_{rec,s}$), A1 and A2 are the fractions of fast and slow inactivating components, and τ1 and τ2 are their time constants $\tau_{rec,f}$ and $\tau_{rec,s}$ respectively.

Dose-responses of channel inhibition by mexiletine were fitted by the Hill equation, as previously described (Zhao et al., 2021a; Zhao et al., 2021b): $\%_i = \%_{i,max}[B]^h/(IC_{50}{}^h+[B]^h)$, where $\%_{i,max}$ is the maximal percentage of channel inhibition by blocker B, h is the Hill coefficient, and IC_{50} is the concentration of mexiletine required for 50% inhibition.

Data and Statistical Analysis

All data were presented as the mean ± SEM. Significance between means was determined by Student's t-test. Electrophysiological parameters ($V_{1/2}$, τ_{dev}, $\tau_{rec,f}$, $\tau_{rec,s}$) were determined from each individual cell and used for comparison with *t*-test. We repeated transfection experiments 3 or 4 times for each group cell, and 2 to 3 sodium currents were recorded in each independent culture. $p < 0.05$ was considered to indicate a statistically significant difference.

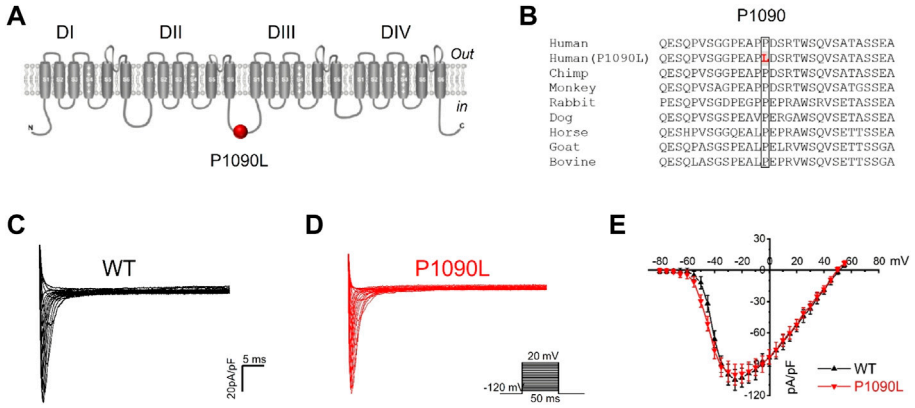

FIGURE 1 | Asian-specific mutation P1090L in the $Na_v1.5$ sodium channel. **(A)**. Topological diagram showing P1090L located in the intracellular loop between the DII-DIII domain of the $Na_v1.5$ channel. **(B)**. $Na_v1.5$ sequence alignment indicates that the P1090 is highly conserved across vertebrate species. **(C,D)**: Representative wild-type (WT) **(C)** and P1090L **(D)** sodium currents. Currents were measured from a holding potential of −120 mV to test potentials ranging between −110 and +60 mV in 5 mV steps. **(E)**. Average peak current-voltage (I-V) relationships for WT channel and P1090L mutation (n = 8 cells in each group, data are presented as the mean ± SEM).

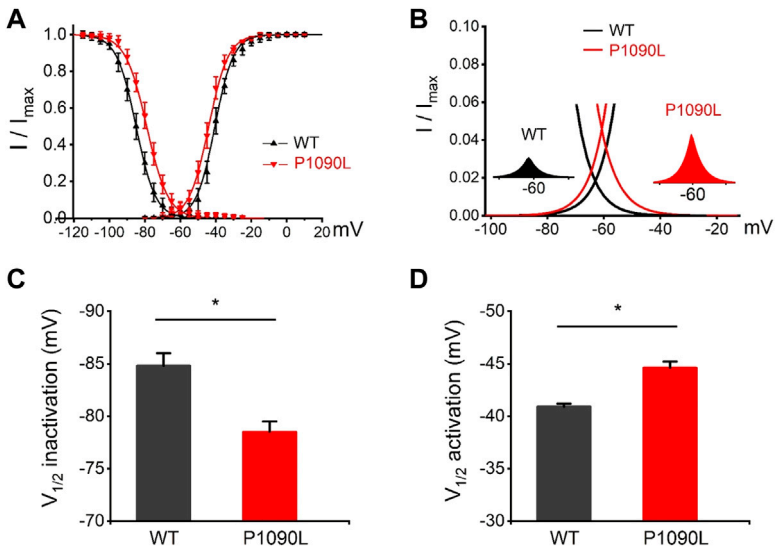

FIGURE 2 | Effects of P1090L mutation on voltage-dependent gating of the $Na_v1.5$ channel. **(A)**. Steady-state activation and inactivation curves of $Na_v1.5$ WT and P1090L mutation. Inactivation currents were elicited to −20 mV following prepulses between −120 and −20 mV in 5 mV steps for 500 ms. Activation currents were measured from a holding potential of −120 mV to test potentials ranging between −110 and +20 mV in 5 mV steps. Curves are Boltzmann fits of the data points (n = 8). **(B)**. The view of the overlapping area between activation and steady-state inactivation was expanded from **(A)**. Left inset shows sodium window current of WT $Na_v1.5$ channel (black). Right inset shows sodium window current of P1090L mutation (red). **(C)**. Summary of $V_{1/2}$ of steady-state inactivation for WT and P1090L channel. **(D)**. Summary of $V_{1/2}$ of voltage-dependent activation for WT and P1090L channel. Data are presented as the mean ± SEM. *p < 0.05.

RESULTS

Effects of P1090L on $Na_v1.5$ Channel Function

The P1090 is located in the intracellular loop between the DII-DIII domain of the $Na_v1.5$ channel (**Figure 1A**). $Na_v1.5$ sequence alignment analysis shows that the native proline (P) at position 1090 is highly conserved across vertebrate species (**Figure 1B**).

Using whole cell patch clamp configuration, we characterized the biophysical properties of the P1090L mutation. The $Na_v1.5$ wild-type (WT) and P1090L mutation in transiently transfected HEK293T cells were studied. We did not observe that P1090L altered the current amplitudes compared with WT (**Figures 1C–E**). However, P1090L shifted voltage dependence of activation to hyperpolarized direction (−44.6 ± 0.6 mV *vs.* −40.9 ± 0.3 mV, n = 8), and shifted voltage dependence of steady-state inactivation to depolarized direction (−78.5 ± 1.0 mV *vs.* −84.8 ±

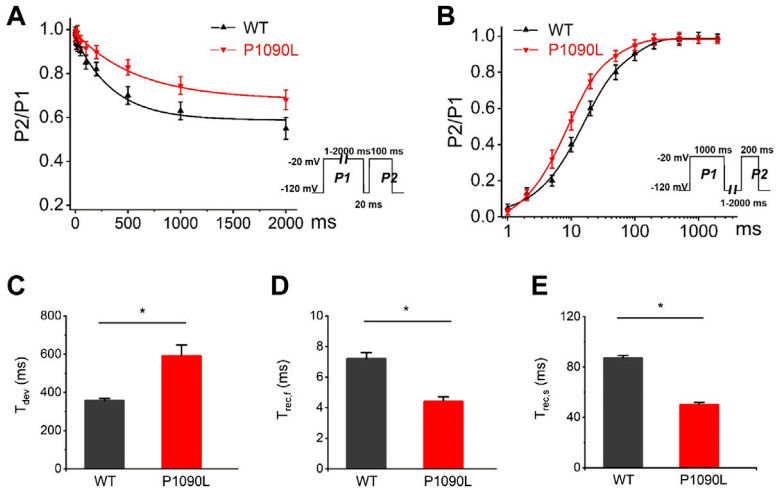

FIGURE 3 | Effects of P1090L mutation on the channel inactivation. **(A)**. Development of inactivation for WT and P1090L mutation was assessed by varying the duration of a conditioning pulse P1 (1–2000 ms) to –20 mV followed by a return to -120 mV for 20 ms followed by a 100 ms test pulse P2 to –20 mV. **(B)**. Recovery of inactivation for WT and P1090L mutation was assessed using insert protocol with a first pulse duration of 1000 ms (P1) and a second pulse of 200 ms (P2) to –20 mV with varying rest intervals from 1 to 2000 ms at –120 mV. Curves in **(A,B)** are exponential function fits of the data points, $n = 8$ in each group. **(C)**. Summary of time constant for development (τ_{dev}) for WT and P1090L channel. **(D)**. Summary of time constant for fast recovery ($\tau_{rec,f}$) for WT and P1090L. **(E)**. Summary of time constant for slow recovery ($\tau_{rec,s}$) for WT and P1090L. Data are presented as the mean ± SEM. *$p < 0.05$.

1.2 mV, $n = 8$) (**Figure 2**). The depolarizing shift in steady-state inactivation and hyperpolarizing shift in activation in P1090L channel produced an overlap of activation and inactivation curves, resulting in a larger "window current" compared with WT channel (**Figure 2B**). This larger window current indicated a gain-of-function mechanism with an increase in sodium channel availability, which might enhance the excitability of myocytes and induce a prolonged ventricular APD underlying LQTS (Wilde and Amin, 2018).

Effects of P1090L on the Channel Inactivation

To determine the effects of P1090L mutation on the process of the inactivation, we assessed the development and recovery of inactivation. The results showed that P1090L increased the time constant for development (τ_{dev}) (591 ± 27 ms *vs.* 357 ± 11 ms, $n = 8$), and decreased fast recovery time constant ($\tau_{rec,f}$) (4.4 ± 0.3 ms *vs.* 7.2 ± 0.4 ms, $n = 8$) and slow recovery time constant ($\tau_{rec,s}$) (50 ± 2 ms *vs.* 87 ± 2 ms, $n = 8$) (**Figure 3**), suggesting that the mutation delayed the process of development and enhanced the recovery from inactivated states of the channel. We also investigated the late sodium current, and P1090L mutation did not show larger persistent inward sodium current compared with WT channel (**Figure 4**).

Mexiletine Inhibited P1090L Current

Since P1090L exhibited an increased window current, we wondered whether we could identify antiarrhythmic drug eliminating the increased window current. The mexiletine was reported to target $Na_v1.5$ mutations and modulate sodium channel function (Ruan et al., 2007; Wang et al., 2015), and it could induce $Na_v1.5$ mutated channels to enter an inactive state to enhance steady-state inactivation process, and decrease channel availability (Sasaki et al., 2004).

We tested the effects of mexiletine on the P1090L peak sodium currents. The P1090L currents were measured prior to and after the addition of the mexiletine, and P1090L mutation currents were significantly inhibited by mexiletine (**Figures 5A,B**). Various concentrations of the drugs were used to generate a dose-response curve, and the IC_{50} value for mexiletine in P1090L mutation was 203 μM (**Figure 5C**). We next used 200 μM to study whether and how mexiletine affected the process of voltage-dependent inactivation in P1090L.

Mexiletine Rescued the Dysfunctional Inactivation of the P1090L Mutation

We observed that the treatment with mexiletine shifted the steady-state inactivation of P1090L currents by around 10 mV to hyperpolarizing direction (−88.2 ± 1.7 mV *vs.* −78.5 ± 1.0 mV, $n = 8$ for control group, $n = 6$ for mexiletine group) with little effect on the channel activation (−46.2 ± 0.8 mV *vs.* −44.6 ± 0.6 mV, $n = 8$ for control, $n = 6$ for mexiletine) (**Figure 6**). The larger window current mediated by P1090L, obtained by plotting the area where steady-state inactivation and activation overlap, was notably reduced by mexiletine (**Figure 6B**). In addition, mexiletine rescued the abnormal inactivation process of the mutation (**Figure 7**). The drug modified development and recovery of inactivation in the mutated channel, and reduced τ_{dev} (436 ± 20 ms *vs.* 591 ± 27 ms, $n = 8$ for control, $n = 6$ for mexiletine), and increased $\tau_{rec,s}$ of P1090L (143 ± 9 ms *vs.* 50 ± 2 ms, $n = 8$ for control, $n = 6$ for mexiletine) (**Figures 7C,E**). These results indicated that mexiletine enhanced P1090L channel

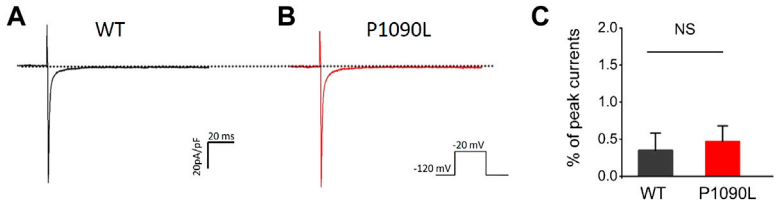

FIGURE 4 | P1090L mutation does not increase the late sodium currents of the $Na_v1.5$ channel. **(A,B)**: Representative wild-type (WT) **(A)** and P1090L **(B)** persistent sodium current traces. Currents were activated by depolarization to −20 mV from a holding potential of −120 mV, and the dash line represented 0 pA. **(C)**. The late sodium currents were measured and normalized to peak currents, n = 6 cells in each group, data are presented as the mean ± SEM. NS, non-significant.

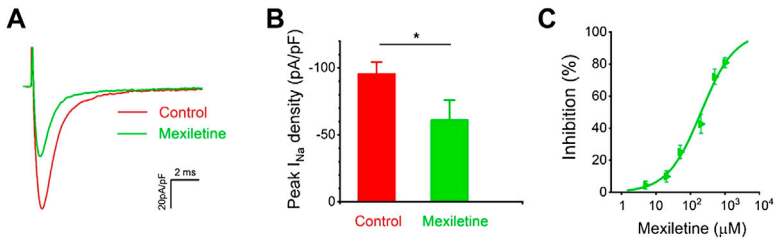

FIGURE 5 | Inhibition of P1090L mutation currents by mexiletine. **(A)**. Representative current traces of P1090L recorded in the absence (Control) and presence of 200 μM mexiletine. Currents were elicited by a test pulse of −20 mV from a holding potential of −120 mV. **(B)**. Quantification of P1090L mutation current densities without (Control) or with the treatment of 200 μM mexiletine. n = 6 for each group, data are presented as the mean ± SEM. *p < 0.05. **(C)**. Dose-dependent effects of mexiletine on P1090L sodium current inhibition (n = 4-6 for each concentration; data are presented as the mean ± SEM). Curves are Hill fits of the data points.

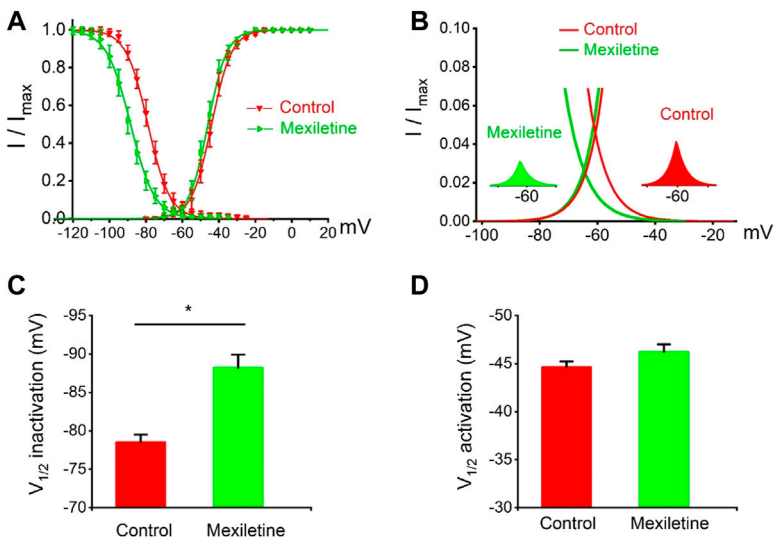

FIGURE 6 | Effects of mexiletine on voltage-dependent gating of the P1090L mutation. **(A)**. Steady-state inactivation and activation curves of P1090L mutation currents in the absence (Control) and presence of 200 μM mexiletine. Inactivation currents were elicited to −20 mV following prepulses between −120 and −20 mV in 5 mV steps for 500 ms. Activation currents were measured from a holding potential of −120 mV to test potentials ranging between −110 and +20 mV in 5 mV steps. Curves are Boltzmann fits of the data points (n = 8 for Control, n = 6 for Mexiletine; data are presented as the means ± SEM). **(B)**. The view of the overlapping area between activation and steady-state inactivation was expanded from **(A)**. Right inset shows P1090L mutation sodium window current without mexiletine (Control), left inset shows P1090L window current in presence of the drug (Mexiletine). **(C)**. Summary of $V_{1/2}$ of steady-state inactivation for control group and mexiletine group. **(D)**. Summary of $V_{1/2}$ of voltage-dependent activation for control and mexiletine. Data are presented as the mean ± SEM. *p < 0.05.

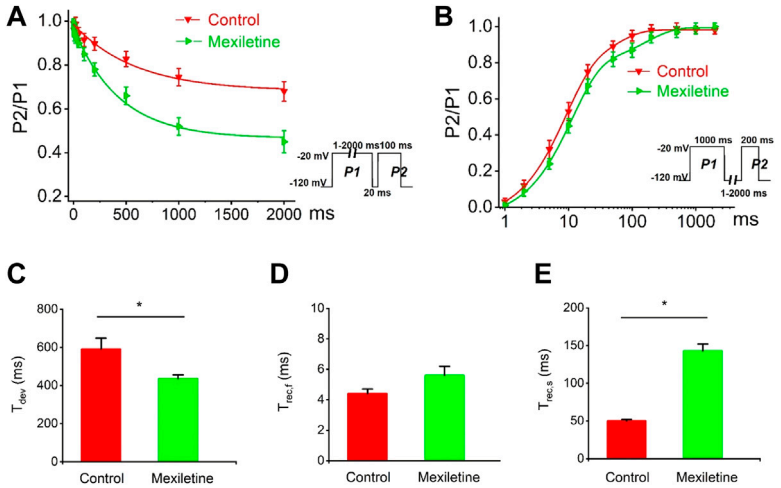

FIGURE 7 | Effects of mexiletine on the development and recovery of inactivation of the P1090L mutation. **(A)**. Development of inactivation for P1090L mutation in the absence (Control) or presence of 200 μM mexiletine was assessed by varying the duration of a conditioning pulse P1 (1–2000 ms) to –20 mV followed by a return to –120 mV for 20 ms followed by a 100 ms test pulse P2 to –20 mV. **(B)**. Recovery of inactivation for P1090L mutation in the presence or absence of mexiletine was assessed using insert protocol with a first pulse duration of 1000 ms (P1) and a second pulse of 200 ms (P2) to –20 mV with varying rest intervals from 1 to 2000 ms at –120 mV. Curves in **(A,B)** are exponential function fits of the data points, $n = 8$ for Control, $n = 6$ for Mexiletine; data are presented as the mean ± SEM. **(C).** Summary of time constant for development (τ_{dev}) for control group and mexiletine group. **(D)**. Summary of time constant for fast recovery ($\tau_{rec,f}$) for control and mexiletine. **(E)**. Summary of time constant for slow recovery ($\tau_{rec,s}$) for control and mexiletine. Data are presented as the mean ± SEM. *$p < 0.05$.

inactivation, stabilized the inactivation gate of the P1090L, and reduced the mutated channel availability.

DISCUSSION

In the present study, we showed that $Na_v1.5$ mutation P1090L linked with LQTS perturbed the process of steady-state inactivation of the channel and generated an enhanced window current that is associated with a gain-of-function mechanism. Treatment with mexiletine rescued the dysfunctional inactivation of the mutation, and decreased the larger window sodium current mediated by P1090L.

The cardiac sodium channel $Na_v1.5$ conducts inward sodium currents initiating the cardiac action potential (Dong et al., 2020). Mutations in $Na_v1.5$ have been linked with inherited arrhythmias such as long QT syndrome (Lai et al., 2005), Brugada Syndrome (Nakajima et al., 2011), atrial fibrillation (Hong et al., 2021). There are two mechanisms proposed to reveal pathophysiological roles of $Na_v1.5$ mutations in arrhythmias (Wilde and Amin, 2018). One is the loss-of function mechanism in which the mutation lacks the molecular function of the wild-type channel. The other is the gain-of-function mechanism in which the mutation changes gene product to confer new or enhanced activity underlying clinical phenotype. The gain-of-function mutations in the $Na_v1.5$ channel normally generate an increase in the window current and/or the late sodium current, resulting in the prolongation of cardiac APD. Previous study reported a negative shift of activation in the Q1077del background for P1090L (Tan et al., 2005). Here we characterized that the P1090L is a gain-of-function mutation, and the mutation presented a larger window current and increased the channel availability. The window current is known as the ionic current flux through ion channels in a voltage range where steady-state inactivation and activation states overlap. The $Na_v1.5$ channel window current usually controls action potential shape in myocytes. However, an enhanced window current may result in severe arrhythmia and heart failure.

Mexiletine is a voltage-gated sodium channel blocker, and the binding sites of mexiletine were proposed to be located at the intracellular side of the channel (Li et al., 2020). Mexiletine belongs to class IB antiarrhythmic agents, previous studies reported that mexiletine exerted a direct effect on LQTS mutations and modified $Na_v1.5$ mutation currents (Kim et al., 2019; Li et al., 2020). A recent study reported differential gating properties of wild-type $Na_v1.5$ and $Na_v1.7$ channels in response to mexiletine and another drug (Wang et al., 2015). Mexiletine did not affect the voltage-dependent activation of the wild-type $Na_v1.5$ channel; however, the steady-state inactivation of the wild-type $Na_v1.5$ was significantly shifted to hyperpolarized direction by mexiletine in dose-dependent manner (Wang et al., 2015). In the present study, we characterized the effects of mexiletine on the mutated channel $Na_v1.5$-P1090L, and showed mexiletine shifted the steady-state inactivation curve of P1090L to a hyperpolarizing direction, the drug rescued an abnormal development and recovery process of the inactivation state in the P1090L mutation. Our results are consistent with previous findings that mexiletine regulated the steady-state inactivation process and induced $Na_v1.5$ mutated channel to enter an inactive state (Sasaki et al., 2004).

In LQTS patients carrying Nav1.5 gain-of-function mutations, an enhanced window current can increase the sodium ion entry into the cells during ventricular diastole. As a result, sodium

currents are more expressed when plateau and repolarization phases last longer, which might explain the clinically observed slow-rate dependent QT prolongation. The larger sodium window current can promote delayed afterdepolarizations, or prolong cardiac action potential inducing the occurrence of early afterdepolarizations. Therefore, a targeted antiarrhythmic drug (AAD) that eliminates the larger window current would reduce the occurrence of arrhythmic events in patients. In the present study, we found that mexiletine reduced the larger window current mediated by the Nav1.5-P1090L mutation. Mechanism-based inhibition of the larger window current by a therapeutic drug would be expected to decrease arrhythmic events in Nav1.5-P1090L patients.

Recent studies on the Nav1.5-P1090L were focused on case reports or genetic analysis, and there was not yet a report on clinical applications of mexiletine in P1090L patients. Like the P1090L, another LQTS mutation Nav1.5-V411M also generates a larger sodium window current associated with the gain-of-function mechanism (Horne et al., 2011). The subsequent clinical investigation reported the consequences of therapy with mexiletine in Nav1.5-V411M patients. Mexiletine was shown to shorten the QT interval and efficaciously reduce arrhythmic events in LQTS patients (Mazzanti et al., 2016).

One limitation of the present study is that we used heterologous expression system to study the race-specific mutation $Na_v1.5$-P1090L. As cardiomyocytes have distinct electrophysiological properties, the *in vitro* method could not capture full spectrum of functional changes of the LQTS-linked mutations. Meanwhile, studies showed that $Na_v1.5$ mutation and other channel are regulators of gene transcriptional networks in cardiomyocytes (Hong et al., 2021; Wu et al., 2022), further studies in patient-specific iPSC-CMs (induced pluripotent stem cell derived cardiomyocytes) will help to explore cellular mechanism of the mutation (Itzhaki et al., 2011).

In summary, we characterized electrophysiological properties of $Na_v1.5$ mutation P1090L linked with LQTS, and showed that mexiletine effectively reduced the enhanced window current generated by P1090L. The results provide insights into the mechanisms by which $Na_v1.5$ mutation causes arrhythmias, and might potentially enable a mechanism-based approach to the treatment of LQTS.

DATA AVAILABILITY STATEMENT

The original contributions presented in the study are included in the article, further inquiries can be directed to the corresponding author.

AUTHOR CONTRIBUTIONS

LH conceived the project and designed the experiments. XW and YL performed experiments. XW and LH wrote the manuscript. All authors revised the manuscript.

FUNDING

This work was supported in part by the National Institutes of Health Grant R01GM139991 (LH) and the American Heart Association Grant 19CDA34630041 (LH).

REFERENCES

Ackerman, M. J., Splawski, I., Makielski, J. C., Tester, D. J., Will, M. L., Timothy, K. W., et al. (2004). Spectrum and Prevalence of Cardiac Sodium Channel Variants Among Black, White, Asian, and Hispanic Individuals: Implications for Arrhythmogenic Susceptibility and Brugada/long QT Syndrome Genetic Testing. *Heart rhythm.* 1, 600–607. doi:10.1016/j.hrthm.2004.07.013

Bankston, J. R., Sampson, K. J., Kateriya, S., Glaaser, I. W., Malito, D. L., Chung, W. K., et al. (2007). A Novel LQT-3 Mutation Disrupts an Inactivation Gate Complex with Distinct Rate-dependent Phenotypic Consequences. *Channels* 1, 273–280. doi:10.4161/chan.4956

Chiu, S.-N., Wu, M.-H., Su, M.-J., Wang, J.-K., Lin, M.-T., Chang, C.-C., et al. (2012). Coexisting Mutations/polymorphisms of the Long QT Syndrome Genes in Patients with Repaired Tetralogy of Fallot Are Associated with the Risks of Life-Threatening Events. *Hum. Genet.* 131, 1295–1304. doi:10.1007/s00439-012-1156-4

Dong, C., Wang, Y., Ma, A., and Wang, T. (2020). Life Cycle of the Cardiac Voltage-Gated Sodium Channel NaV1.5. *Front. Physiol.* 11, 609733. doi:10.3389/fphys.2020.609733

Grant, A. O., Carboni, M. P., Neplioueva, V., Starmer, C. F., Memmi, M., Napolitano, C., et al. (2002). Long QT Syndrome, Brugada Syndrome, and Conduction System Disease Are Linked to a Single Sodium Channel Mutation. *J. Clin. Invest.* 110, 1201–1209. doi:10.1172/jci0215570

Hong, L., Zhang, M., Ly, O. T., Chen, H., Sridhar, A., Lambers, E., et al. (2021). Human Induced Pluripotent Stem Cell-Derived Atrial Cardiomyocytes Carrying an SCN5A Mutation Identify Nitric Oxide Signaling as a Mediator of Atrial Fibrillation. *Stem Cell Rep.* 16, 1542–1554. doi:10.1016/j.stemcr.2021.04.019

Hong, L., Zhang, M., Sridhar, A., and Darbar, D. (2020). Pathogenic Mutations Perturb Calmodulin Regulation of Nav1.8 Channel. *Biochem. Biophys. Res. Commun.* 533 (1), 168–174. doi:10.1016/j.bbrc.2020.08.010

Horne, A. J., Eldstrom, J., Sanatani, S., and Fedida, D. (2011). A Novel Mechanism for LQT3 with 2:1 Block: a Pore-Lining Mutation in Nav1.5 Significantly Affects Voltage-Dependence of Activation. *Heart rhythm.* 8, 770–777. doi:10.1016/j.hrthm.2010.12.041

Itzhaki, I., Maizels, L., Huber, I., Zwi-Dantsis, L., Caspi, O., Winterstern, A., et al. (2011). Modelling the Long QT Syndrome with Induced Pluripotent Stem Cells. *Nature* 471, 225–229. doi:10.1038/nature09747

Iwasa, H., Itoh, T., Nagai, R., Nakamura, Y., and Tanaka, T. (2000). Twenty Single Nucleotide Polymorphisms (SNPs) and Their Allelic Frequencies in Four Genes that Are Responsible for Familial Long QT Syndrome in the Japanese Population. *J. Hum. Genet.* 45, 182–183. doi:10.1007/s100380050207

Kapa, S., Tester, D. J., Salisbury, B. A., Harris-Kerr, C., Pungliya, M. S., Alders, M., et al. (2009). Genetic Testing for Long-QT Syndrome. *Circulation* 120, 1752–1760. doi:10.1161/circulationaha.109.863076

Kim, H.-J., Kim, B.-G., Park, J. E., Ki, C.-S., Huh, J., Youm, J. B., et al. (2019). Characterization of a Novel LQT3 Variant with a Selective Efficacy of Mexiletine Treatment. *Sci. Rep.* 9, 12997. doi:10.1038/s41598-019-49450-0

Kim, I. H., Hevezi, P., Varga, C., Pathak, M. M., Hong, L., Ta, D., et al. (2014). Evidence for Functional Diversity between the Voltage-Gated Proton Channel Hv1 and its Closest Related Protein HVRP1. *PLoS One* 9, e105926. doi:10.1371/journal.pone.0105926

Lai, L.-P., Su, Y.-N., Chiang, F.-T., Juang, J.-M., Liu, Y.-B., Ho, Y.-L., et al. (2005). Denaturing High-Performance Liquid Chromatography Screening of the Long QT Syndrome-Related Cardiac Sodium and Potassium Channel Genes and Identification of Novel Mutations and Single Nucleotide Polymorphisms. *J. Hum. Genet.* 50, 490–496. doi:10.1007/s10038-005-0283-3

Li, G., Woltz, R. L., Wang, C.-y., Ren, L., He, P.-x., Yu, S.-d., et al. (2020). Gating Properties of Mutant Sodium Channels and Responses to Sodium Current Inhibitors Predict Mexiletine-Sensitive Mutations of Long QT Syndrome 3. *Front. Pharmacol.* 11, 1182. doi:10.3389/fphar.2020.01182

Mazzanti, A., Maragna, R., Faragli, A., Monteforte, N., Bloise, R., Memmi, M., et al. (2016). Gene-Specific Therapy with Mexiletine Reduces Arrhythmic Events in Patients with Long QT Syndrome Type 3. *J. Am. Coll. Cardiol.* 67, 1053–1058. doi:10.1016/j.jacc.2015.12.033

Nakajima, T., Kaneko, Y., Saito, A., Irie, T., Tange, S., Iso, T., et al. (2011). Identification of Six Novel SCN5A Mutations in Japanese Patients with Brugada Syndrome. *Int. Heart J.* 52, 27–31. doi:10.1536/ihj.52.27

Napolitano, C., Priori, S. G., Schwartz, P. J., Bloise, R., Ronchetti, E., Nastoli, J., et al. (2005). Genetic Testing in the Long QT Syndrome. *JAMA* 294, 2975–2980. doi:10.1001/jama.294.23.2975

Ruan, Y., Liu, N., Bloise, R., Napolitano, C., and Priori, S. G. (2007). Gating Properties of SCN5A Mutations and the Response to Mexiletine in Long-QT Syndrome Type 3 Patients. *Circulation* 116, 1137–1144. doi:10.1161/circulationaha.107.707877

Sasaki, K., Makita, N., Sunami, A., Sakurada, H., Shirai, N., Yokoi, H., et al. (2004). Unexpected Mexiletine Responses of a Mutant Cardiac Na+ Channel Implicate the Selectivity Filter as a Structural Determinant of Antiarrhythmic Drug Access. *Mol. Pharmacol.* 66, 330–336. doi:10.1124/mol.66.2.330

Shan, L., Makita, N., Xing, Y., Watanabe, S., Futatani, T., Ye, F., et al. (2008). SCN5A Variants in Japanese Patients with Left Ventricular Noncompaction and Arrhythmia. *Mol. Genet. Metabolism* 93, 468–474. doi:10.1016/j.ymgme.2007.10.009

Tan, B.-H., Valdivia, C. R., Rok, B. A., Ye, B., Ruwaldt, K. M., Tester, D. J., et al. (2005). Common Human SCN5A Polymorphisms Have Altered Electrophysiology when Expressed in Q1077 Splice Variants. *Heart rhythm.* 2, 741–747. doi:10.1016/j.hrthm.2005.04.021

Wang, Y., Mi, J., Lu, K., Lu, Y., and Wang, K. (2015). Comparison of Gating Properties and Use-dependent Block of Nav1.5 and Nav1.7 Channels by Anti-arrhythmics Mexiletine and Lidocaine. *PLoS One* 10, e0128653. doi:10.1371/journal.pone.0128653

Ware, J. S., Walsh, R., Cunningham, F., Birney, E., and Cook, S. A. (2012). Paralogous Annotation of Disease-Causing Variants in Long QT Syndrome Genes. *Hum. Mutat.* 33, 1188–1191. doi:10.1002/humu.22114

Wilde, A. A. M., and Amin, A. S. (2018). Clinical Spectrum of SCN5A Mutations. *JACC Clin. Electrophysiol.* 4, 569–579. doi:10.1016/j.jacep.2018.03.006

Wu, X., and Hong, L. (2021). Calmodulin Interactions with Voltage-Gated Sodium Channels. *Int. J. Mol. Sci.* 22, 9798. doi:10.3390/ijms22189798

Wu, X., Li, Y., Maienschein-Cline, M., Feferman, L., Wu, L., and Hong, L. (2022). RNA-Seq Analyses Reveal Roles of the HVCN1 Proton Channel in Cardiac pH Homeostasis. *Front. Cell Dev. Biol.* 10, 860502. doi:10.3389/fcell.2022.860502

Zhang, Y., Chang, B., Hu, S., Wang, D., Fang, Q., Huang, X., et al. (2008). Single Nucleotide Polymorphisms and Haplotype of Four Genes Encoding Cardiac Ion Channels in Chinese and Their Association with Arrhythmia. *Ann. Noninv Electrocard* 13, 180–190. doi:10.1111/j.1542-474x.2008.00220.x

Zhao, C., Hong, L., Riahi, S., Lim, V. T., Tobias, D. J., and Tombola, F. (2021b). A Novel Hv1 Inhibitor Reveals a New Mechanism of Inhibition of a Voltage-Sensing Domain. *J. Gen. Physiol.* 153, e202012833. doi:10.1085/jgp.202012833

Zhao, C., Hong, L., Galpin, J. D., Riahi, S., Lim, V. T., Webster, P. D., et al. (2021a). HIFs: New Arginine Mimic Inhibitors of the Hv1 Channel with Improved VSD-Ligand Interactions. *J. Gen. Physiol.* 153, e202012832. doi:10.1085/jgp.202012832

Conflict of Interest: The authors declare that the research was conducted in the absence of any commercial or financial relationships that could be construed as a potential conflict of interest.

Publisher's Note: All claims expressed in this article are solely those of the authors and do not necessarily represent those of their affiliated organizations, or those of the publisher, the editors and the reviewers. Any product that may be evaluated in this article, or claim that may be made by its manufacturer, is not guaranteed or endorsed by the publisher.